

## RXTE OBSERVATION OF CYGNUS X-1: SPECTRAL ANALYSIS

JAMES B. DOVE<sup>1,2</sup>, JÖRN WILMS<sup>3,1</sup>, MICHAEL A. NOWAK<sup>1</sup>, BRIAN A. VAUGHAN<sup>4</sup>, AND MITCHELL C. BEGELMAN<sup>1,2</sup>

*Draft version December 2, 2024*

### ABSTRACT

We present the results of the spectral analysis of the broad-band spectrum of Cygnus X-1 from 5.5 to 200 keV, using data from a 10ksec observation by the *Rossi X-ray Timing Explorer*. The spectrum is well described by a power law with a photon index  $\Gamma = 1.43 \pm 0.02$ , modified by an exponential cut-off with an  $e$ -folding energy  $E_f = 152_{-7}^{+8}$  keV, and a weak soft excess component that can be modeled as a thermal blackbody having a temperature  $kT_{\text{BB}} = 1.0 \pm 0.1$  keV. The inclusion of a reflection component does not improve the fit. We apply the accretion disk corona models of Dove, Wilms & Begelman (1997) — where the temperature of the corona is determined self-consistently — to the observation. A slab-geometry accretion disk corona model, where a hot corona sandwiches a cold disk, predicts a spectrum that is too soft to explain the observations. On the other hand, a spherical corona (with an optical depth  $\tau = 2.1 \pm 0.1$  and an average temperature  $kT_C = 66 \pm 3$  keV) that is surrounded by an exterior cold disk provides a good description of the data. Such “photon-starved” coronal geometries are therefore more promising for explaining the accretion process of Cygnus X-1.

*Subject headings:* stars: individual (Cygnus X-1) – methods: data analysis – accretion – radiation mechanisms: nonthermal – X-rays: stars – black hole physics

### 1. INTRODUCTION

Cygnus X-1 is one of the most firmly established persistent galactic black hole candidates (BHCs). Since it is also one of the brightest BHCs, the study of its X-ray spectrum can help reveal the physical conditions of the inner region around accreting compact objects. The X-ray spectrum of Cyg X-1 while in the hard (i.e., low) state can be roughly described by a power-law with a photon-index  $\Gamma \sim 1.65$ , modified by an exponential cutoff with an  $e$ -folding energy  $E_f \sim 150$  keV (Ebisawa 1997; Gierliński et al. 1997, and references therein). The spectral shape of this form is naturally explained by Comptonization of low-energy seed photons by a semi-relativistic corona (Sunyaev & Trümper 1979; Titarchuk 1994). Below about 10 keV, there is evidence for a soft-excess, usually interpreted as thermal radiation from a cold accretion disk having a temperature  $kT_{\text{BB}} \sim 0.2$ – $0.7$  keV (Bałucińska-Church et al. 1995; Ebisawa 1997). In addition, the spectrum is usually found to contain weak iron line features at  $\approx 6.4$  keV and a slight hardening above 10 keV, often interpreted as being due to Compton reflection (Barr, White & Page 1985; Ebisawa 1997 and references therein).

The combination of a Comptonization continuum and reprocessing features has been interpreted as being due to an accretion disk corona (ADC). The geometric configuration of the corona and the cold disk, however, is still unclear. In most recent work, the geometry has been assumed to be a slab-like cold accretion disk embedded between two hot coronae (Haardt, Maraschi & Ghisellini 1996; Haardt et al. 1993 and references therein).

Recently, however, evidence has been presented, showing that ADC models with a slab geometry suffer from several problems, making them less likely to be the appropriate models for explaining the high-energy radiation of BHCs. Gierliński et al. (1997) analyzed simultaneous *Ginga*-OSSE data of Cyg X-1 and found that the strength of the reflection component is too small to be consistent with a slab geometry. Using a non-simultaneous broad-band spectrum of Cyg X-1, we previously argued that our self-consistent ADC corona models with a slab geometry (in which the coronal temperature is not a free parameter but is determined by balancing Compton cooling with viscous dissipation) could not have a high enough temperature to explain both the observed power-law and exponential cutoff (Dove, Wilms & Begelman 1997; Dove et al. 1997; Wilms et al. 1997). Moreover, the luminosity of the disk expected due to reprocessing is comparable to the coronal luminosity, and therefore the predicted soft-excess component is much stronger than that observed (Dove et al. 1997; Gierliński et al. 1997).

Most of the problems cited above are due to the cold disk of the slab-like ADC model having a covering fraction of unity (i.e., all downward directed coronal radiation is reprocessed in the cold disk). ADCs having a geometry with a smaller covering fraction have weaker reprocessing features and are less efficiently Compton cooled, thereby allowing for higher coronal temperatures. An example is a hot coronal sphere that is surrounded by an exterior cold accretion disk (called the “sphere+disk geometry” henceforth), similar to the two-temperature disk model of Shapiro, Lightman & Eardley (1976) and to ad-

<sup>1</sup>JILA, University of Colorado and National Institute of Standards and Technology, Campus Box 440, Boulder, CO 80309-0440; {dove,mnowak}@rocinate.colorado.edu, mitch@jila.colorado.edu

<sup>2</sup>Department of Astrophysical and Planetary Sciences, University of Colorado, Boulder, CO 80309-0391

<sup>3</sup>Institut für Astronomie und Astrophysik, Abt. Astronomie, Waldhäuser Str. 64, D-72076 Tübingen, Germany; wilms@astro.uni-tuebingen.de

<sup>4</sup>Space Radiation Laboratory, California Institute of Technology, 220-47 Downs, Pasadena, CA 91125; brian@srl.caltech.edu

vection dominated models (Abramowicz et al. 1995; Chen 1995; Narayan & Yi 1994). Based on non-simultaneous BBXRT, Mir-TTM, Mir-HEXE, and OSSE data, we have shown that the sphere+disk ADC model can explain the observed spectrum of Cyg X-1 for energies between about 1 keV and 1 MeV (Dove et al. 1997).

In this letter, we analyze the broad-band spectrum of Cyg X-1 from 5.5 to 200 keV, using data from the *Ross X-ray Timing Explorer* (RXTE). The simultaneity of this broad-band observation allows us to place stronger constraints on the coronal parameters than previously possible. In §2, we describe the observations performed and the procedures used in the data analysis. In §3, we give the results from spectral modeling of the Cyg X-1 spectrum using both “standard” simplified models as well as our self-consistent ADC models. In §4 the results of these fits are discussed.

## 2. OBSERVATIONS AND DATA ANALYSIS

RXTE observed Cyg X-1 for a total of 22.5 ksec on 1996 October 23 and 24. For the analysis presented here, we use data from the proportional counter array (PCA) and the high energy X-ray timing experiment (HEXTE). The PCA consists of five Xe proportional counters with a total effective area of about 6500 cm<sup>2</sup> (Zhang et al. 1993), while HEXTE consists of two clusters of NaI(Tl)/CsI scintillation counters with a total effective area of about 1400 cm<sup>2</sup> (Gruber et al. 1996). For both instruments, only data where the source was observed at elevations higher than 10° above the spacecraft horizon were used. Due to missing standard-mode PCA data, we have used only the first 10 ksec of the observation. This duration is sufficient for the spectral analysis, as the PCA count-rate is high ( $\approx 4300$  cps).

For the extraction of the PCA data, we used the standard RXTE ftools, version 4.0. We used version 1.5 of the background estimator program, in which activation due to the South Atlantic Anomaly and an estimate for the internal background based on the measurement of the rate of Very Large Events within the PCA are taken into account. To this estimation, the measured X-ray background is added. The comparison of the modeled background spectrum to the background measured within PCA during the Earth looking phases of the observation (defined by an elevation  $< -5^\circ$ ) indicates that the background model count-rate has an uncertainty of 5 to 10%. The use of the background model is still preferable to using the Earth occultation data because the latter method cannot estimate the variation of the background due to the variation of the rigidity of the Earth’s magnetic field during on-source time intervals.

For the spectral analysis of the PCA data, version 2.6.1 of the PCA response matrix was used (for an overview of the PCA calibration issues, see Jahoda et al. 1996). The PCA response matrix is fairly well understood, except around the Xenon K- and L- edges at 34.5 and 5.5 keV, respectively. Rapid changes in the effective area of the detector result in an uncertainty of about 5% in the response at energies below 5.5 keV. These data were therefore ignored. In addition, due to the uncertainty in the

response-matrix at 34.5 keV and the problems of the background estimation, the PCA data above 25 keV were also ignored. HEXTE, however, provides reliable data at these energies. To account for the additional uncertainties in the PCA response matrix, a 2% systematic error was added to all PCA data.

Software provided by the HEXTE instrument group was used for the extraction of the HEXTE data and subsequent dead-time corrections. Since HEXTE is source-background swapping, the background is not a problem in the data analysis. We used the HEXTE response matrices, released 1997 March 20. Only data above 20 keV were used due to the uncertainty of the response matrix below these energies. At high energies, the spectrum was cut at 200 keV. To ensure good statistical accuracy above 50 keV, the spectrum was rebinned by a factor of 3 for channels between 50 and 100 keV, and by a factor of 10 for higher channels.

## 3. SPECTRAL ANALYSIS

### 3.1. Standard Models

Spectral fitting was first performed using standard models: a power-law, a power-law with an exponential cutoff, a power-law with an exponential cutoff plus a cold reflection component, and thermal Comptonization models were used. We fixed the low-energy absorption to an equivalent cold Hydrogen column of  $N_{\text{H}} = 6 \times 10^{21}$  cm<sup>-2</sup>, the value suggested by soft X-ray and interstellar reddening measurements of HDE 226868 (Wu et al. 1982; Bahucińska & Hasinger 1991). The results of the spectral fits are given in table 1<sup>1</sup>.

A pure power law model does not describe the data well, especially at energies  $\gtrsim 70$  keV. A better approximation is given by a power-law with an exponential cutoff. The value for the  $e$ -folding energy,  $E_f$ , is well constrained due to the quality of the HEXTE data. The analysis of the residuals of this fit indicates the presence of a soft excess at low energies. Adding a black-body component to the model improves the quality of the fit, resulting in a good description of the data over the whole energy range ( $\chi_{\text{red}}^2 = 0.84$ ). The addition of a reflection component to this model *does not* improve the quality of the fit. In fact, the strength of the reflection feature is found to be very weak: the fraction of the incident radiation that is Compton reflected by the cold matter is  $f = 0.07_{-0.06}^{+0.06}$ .

We note that our fits do not require the addition of an Fe  $K\alpha$  line. This result is probably in agreement with the results based on four days of ASCA observations presented by Ebisawa (1997), who found a comparably weak Fe line with an equivalent width  $\text{EW} \lesssim 30$  eV. Simulations suggest that our observation would be sensitive to a Fe line with  $\text{EW} > 20$  eV if the sensitivity were not reduced by the calibration problems at low energies. Due to these problems, however, line features having an  $\text{EW} \lesssim 100$  eV are currently undetectable.

Thermal Comptonization provides a physical model for the observed power-law spectrum of Cyg X-1. Applying the model of Titarchuk (1994) to the data, we find that a thermal Comptonization spectrum, resulting from

<sup>1</sup>To account for the known discrepancies in the relative normalization of PCA and HEXTE, we introduced a multiplicative constant in the spectral models that represents the relative normalization between the data-sets. the relative normalization between HEXTE and PCA was always found to be  $0.70 \pm 0.01$ . The relative normalization constant is therefore not listed in table 1.

a spherical geometry with  $\tau \approx 3.7$  and  $kT_C \approx 39$  keV, can give an acceptable description of the data, although the model underestimates the flux at energies  $\gtrsim 150$  keV. A semi-relativistic, optically thin model, for either a slab geometry or a spherical geometry, was unable to explain the data.

Although the traditional models are quite successful in describing the observed broad band spectrum of Cyg X-1, in most cases the models do not yield a physical interpretation of the emitting mechanisms responsible for the production of the high-energy radiation. In the next section, therefore, we apply our ADC models to the observed data.

### 3.2. Accretion Disk Corona models

For both a slab-like ADC model and the sphere+disk ADC model, we have computed grids of spectra using a non-linear Monte Carlo scheme based on the code of Stern et al. (1995) and modified by Dove, Wilms & Begelman (1997) and Dove et al. (1997). The free parameters of the model are the seed optical depth  $\tau_e$ , i.e. the optical depth of the corona excluding the contribution from electron-positron pairs, and the heating rate of the ADC. For a given heating rate, the temperature structure of the corona is determined by balancing Compton cooling with heating, where the heating rate is assumed to be uniformly distributed. The  $e^-e^+$ -pair opacity is given by balancing photon-photon pair production with annihilation. Reprocessing of coronal radiation in the cold accretion disk is also treated numerically<sup>2</sup>. The outer radius of the cold disk is assumed to be five times the radius of the coronal sphere. The model spectra have been implemented into the data reduction software *XSPEC* (Arnaud 1996) for use in spectral fitting. The grids of model spectra and the interpolation routines, based on Delaunay triangularization, are available upon request.

Slab-corona models do not result in good fits, as the predicted spectra are always much softer than the observed spectrum ( $\chi_{\text{red}} \sim 80$ ). This result is consistent with our previous findings based on non-simultaneous data (Dove et al. 1997). The sphere+disk ADC model, however, does provide a good description to the data (see table 1). The best-fit model and the ratio between the data and the model are shown in Fig. 1. The formal  $\chi^2$ -value of our best-fit sphere+disk model is slightly larger than the values found for some of the models discussed in §3.1. This is in part due to the statistical errors associated with Monte Carlo models, where computational time constraints prohibit the generation of models with a very high signal to noise ratio. We note, however, that our model only contains two free parameters, and contrary to the analytical Comptonization model, our ADC model is able to describe the exponential tail of the spectrum. We also note that the sphere+disk models in which the inner temperature of the disk is  $kT_{\text{BB}} = 800$  eV, a temperature consistent with the best-fit temperature in the *plexp* model, predict much more of a soft-excess than observed.

<sup>2</sup>One improvement to the sphere+disk model, not discussed in Dove et al. (1997), is the treatment of thermal radiation emitted by the accretion disk. Currently, the temperature of the accretion disk is assumed to be  $T_{\text{BB}} \propto (R/R_C)^{-3/4}$ , where  $R$  is the disk radius and  $R_C$  is the radius of the coronal sphere. The implicit flux of the disk (i.e., the radiation emitted due to viscous energy dissipation and not due to reprocessing of coronal radiation) is given by  $F(R) = \sigma T^4(R)$ , and the spectral shape is determined by the *local* disk temperature (a superposition of thermal Planckian distributions).

## 4. DISCUSSION AND CONCLUSIONS

We have applied a variety of spectral models to an RXTE observation of Cyg X-1. We find that the observed spectrum between 5.5 and 200 keV is well described by a power-law with a photon index  $\Gamma = 1.42 \pm 0.02$  modified by an exponential tail with an  $e$ -folding energy  $E_f \approx 150$  keV, and a thermal component having a temperature  $kT_{\text{BB}} \approx 1$  keV. The measured value of  $\Gamma$  is lower than those found in previous broad-band analyses, which find a  $\Gamma \sim 1.65$ . (Gierliński et al. 1997; Döbereiner et al. 1994). In addition, the observed strength of the Compton reflection feature is weak, as the best-fit covering fraction is found to be  $\approx 0.07$ , a value considerably lower than the  $f \approx 0.3$  found by Gierliński et al. (1997).

We did find that, for the PCA data alone, the spectrum could be described by a power-law with a photon index  $\Gamma \sim 1.7$ , a value more consistent with previous values found for this energy range (Ebisawa 1997; Done et al. 1992, and references therein). However, by applying the reflection model to only the PCA data, we still find no evidence for Compton reflection. An open question is whether these somewhat unique properties are due in part to the transition from the “soft” state to the “hard” state that ended only two weeks prior to our observation (cf. Cui et al. 1997 for a discussion of the soft-state properties of Cyg X-1).

Slab-like ADC models are unable to explain the observed hard power-law and the small amount of reprocessing, consistent with the results of Dove et al. (1997), Gierliński et al. (1997), and Poutanen, Krolik & Felix (1997). In contrast, the sphere+disk ADC models *can* explain the observed data. Contrary to the results of Gierliński et al. (1997), we were able to fit the high-energy tail with a *single* Comptonizing component. This result might be due to the  $\sim 15\%$  variation of the coronal temperature (due to the non-uniform radiation field and the corresponding non-uniform Compton cooling rate) in our models.

Due to the data’s broad energy range, the physical properties of the corona are well constrained. However, it is premature to claim that the sphere+disk configuration is indeed the appropriate geometry. Other, albeit unknown, geometries in which a small fraction of coronal radiation is reprocessed by the disk, may also be able to describe the data. The spectral features due to the reprocessing of coronal radiation in the cold disk (i.e., the Fe K $\alpha$  fluorescence line, the Compton reflection “bump,” and the soft-excess due to thermalization of the coronal radiation) occur for energies between  $\sim 0.1$ –20 keV, and different geometries will predict slightly different reprocessing features. Since we ignored data below 5.5 keV, we were not able to reasonably constrain the model parameters which deal with the soft-excess, nor can the strength of the iron line be directly measured. Therefore, more low energy data are needed to further constrain ADC models for Cyg X-1. However,

since previous observations all show only a very weak soft excess and low equivalent widths, we consider it a triumph of the sphere+disk configuration that such features are consistent with previous observations.

Additional constraints to the ADC models can come from measurements of time-lags and the temporal coherence between several energy bands from the source. These measurements can be compared with the time-lags and coherence function predicted using the physical parameters of the geometry found from spectral fitting (Vaughan & Nowak 1997; Nowak & Vaughan 1996). Only a geometry in which both the spectral and the temporal data can

be explained should be considered a valid candidate for Cyg X-1. We are planning to use such an approach in a forthcoming paper.

We acknowledge the help of D. Gruber with the HEXTE data analysis and useful discussions with I. Kreykenbohm, Ch. Reynolds, and R. Staubert. This work has been financed by NSF grants AST91-20599, AST95-29175, INT95-13899, NASA Grant NAG5-2026, NAG5-3225, NAGS-3310, DARA grant 50OR92054, and by a travel grant to J.W. from the DAAD.

#### REFERENCES

- Abramowicz, M., Chen, X., Kato, S., Lasota, J. P., & Regev, O., 1995, *ApJ*, 438, L37
- Arnaud, K. A., 1996, in *Astronomical Data Analysis Software and Systems V*, ed. J. H. Jacoby, J. Barnes, (San Francisco: Astron. Soc. Pacific), 17
- Balucińska-Church, M., Belloni, T., Church, M. J., & Hasinger, G., 1995, *A&A*, 302, L5
- Balucińska, M., & Hasinger, G., 1991, *A&A*, 241, 439
- Barr, P., White, N. E., & Page, C. G., 1985, *MNRAS*, 216, 65p
- Chen, X., 1995, *MNRAS*, 275, 641
- Cui, W., Heindl, W. A., Rothschild, R. E., Zhang, S. N., Jahoda, K., & Focke, W., 1997, *ApJ*, 474, L57
- Döbereiner, S., et al., 1994, *A&A*, 287, 105
- Done, C., Mulchaey, J. S., Mushotzky, R. F., & Arnaud, K. A., 1992, *ApJ*, 395, 275
- Dove, J. B., Wilms, J., & Begelman, M. C., 1997, *ApJ*, 487, in press
- Dove, J. B., Wilms, J., Maisack, M. G., & Begelman, M. C., 1997, *ApJ*, 487, in press
- Ebisawa, K., 1997, *Adv. Space Res.*, 19, 5
- Gierliński, M., Zdziarski, A. A., Done, C., Johnson, W. N., Ebisawa, K., Ueda, Y., Haardt, F., & Philips, B. F., 1997, *MNRAS*, in press
- Gruber, D. E., Blanco, P. R., Heindl, W. A., Pelling, M. R., Rothschild, R. E., & Hink, P. L., 1996, *A&AS*, 120, C641
- Haardt, F., Done, C., Matt, G., & Fabian, A. C., 1993, *ApJ*, 411, L95
- Haardt, F., Maraschi, L., & Ghisellini, G., 1996, *ApJ*, 476, 670
- Hua, X.-M., & Titarchuk, L., 1995, *ApJ*, 449, 188
- Jahoda, K., et al., 1996, *BAAS*, 189, 09.06
- Magdziarz, P., & Zdziarski, A. A., 1995, *MNRAS*, 273, 837
- Narayan, R., & Yi, I., 1994, *ApJ*, 428, L13
- Nowak, M. A., & Vaughan, B. A., 1996, *MNRAS*, 280, 227
- Poutanen, J., Krolik, J. H., & Felix, R., 1997, *MNRAS*, submitted
- Shapiro, S. L., Lightman, A. P., & Eardley, D., 1976, *ApJ*, 204
- Stern, B. E., Begelman, M. C., Sikora, M., & Svensson, R., 1995, *MNRAS*, 272, 291
- Sunyaev, R. A., & Trümper, J., 1979, *Nature*, 279, 506
- Titarchuk, L., 1994, *ApJ*, 434, 570
- Vaughan, B. A., & Nowak, M. A., 1997, *ApJ*, 474, L43
- Wilms, J., Dove, J., Staubert, R., & Begelman, M. C., 1997, in *The Transparent Universe*, ed. C. Winkler, T. J.-L. Courvoisier, P. Durouchoux, (Noordwijk: ESA Publications Division), 233
- Wu, C.-C., Eaton, J. A., Holm, A. V., Milgrom, M., & Hammerschlag-Hensberge, G., 1982, *PASP*, 94, 149
- Zhang, W., Giles, A. B., Jahoda, K., Soong, Y., Swank, J. H., & Morgan, E. H., 1993, in *EUV, X-Ray, and Gamma-Ray Instrumentation for Astronomy IV*, ed. O. H. Siegmund, (Bellingham, WA: SPIE), 324

TABLE 1  
RESULTS OF SPECTRAL FITTING TO CYG X-1.

Model	$\Gamma$	$A_{\text{PL}}$	$E_f$ [keV]	$kT_{\text{BB}}$ [keV]	$A_{\text{BB}}$ $10^{-2}$	$f$ $10^{-2}$	$kT_{\text{C}}$ keV	$\tau_e$	$A_{\text{C}}$	$\chi^2/\text{dof}$
pl	1.75	1.92	...	...	...	...	...	...	...	1403/156
plexp	$1.53^{+0.01}_{-0.01}$	$1.18^{+0.03}_{-0.04}$	$214^{+12}_{-11}$	...	...	...	...	...	...	429/155
plexp+bb	$1.42^{+0.02}_{-0.02}$	$0.89^{+0.04}_{-0.04}$	$151^{+8}_{-7}$	$1.1^{+0.3}_{-0.3}$	$2.0^{+0.3}_{-0.3}$	...	...	...	...	130/153
pextrav	$1.56^{+0.03}_{-0.03}$	$1.25^{+0.07}_{-0.06}$	$260^{+40}_{-40}$	...	...	$7^{+6}_{-6}$	...	...	...	424/154
pextrav+bb	$1.45^{+0.03}_{-0.03}$	$0.93^{+0.06}_{-0.05}$	$170^{+24}_{-18}$	$1.2^{+0.1}_{-0.1}$	$1.9^{+0.3}_{-0.2}$	$6.5^{+7.0}_{-6.4}$	...	...	...	127/152
comptt+bb	...	...	...	$0.9^{+0.1}_{-0.1}$	$1.6^{+0.7}_{-0.4}$	...	$39^{+1}_{-1}$	$3.7^{+0.1}_{-0.1}$	$0.090^{+0.004}_{-0.004}$	244/153
s+d	...	...	...	...	...	...	$65.7^{+3.3}_{-3.3}$	$2.1^{+0.1}_{-0.1}$	$6.48^{+0.06}_{-0.05}$	152/155

NOTE.— $N_{\text{H}}$  was fixed at  $6 \times 10^{21} \text{ cm}^{-2}$ . Uncertainties given are at the 90% level for one interesting parameter ( $\Delta\chi^2 = 2.7$ ). pl: power-law with photon-index  $\Gamma$  and normalization  $A_{\text{PL}}$  (photon-flux at 1 keV); plexp: power-law with exponential cutoff [ $A_{\text{PL}} E^{-\Gamma} \exp(-E/E_f)$ ]; bb: black body with temperature  $kT_{\text{BB}}$ ; the normalization  $A_{\text{BB}}$  is defined in units of  $L_{39}/R_{10}^2$  where  $L_{39}$  is the luminosity in units of  $10^{39} \text{ erg/s}$  and  $R_{10}$  is the distance in units of 10 kpc; pextrav: power-law with exponential cutoff reflected off cold matter (using Green's functions of Magdziarz & Zdziarski 1995),  $f$  is the ratio between the incident and the reflected flux; comptt: Comptonization spectrum after Hua & Titarchuk (1995) and Titarchuk (1994), with a coronal temperature of  $kT_{\text{C}}$  and total optical depth  $\tau_e$ , seed-photon temperature is 10 eV; s+d: ADC model with sphere+disk geometry, optical depth of the sphere is  $\tau_e$ , temperature of the sphere is  $kT_{\text{C}}$ , the temperature profile of the cold disk is  $kT_{\text{BB}}(R) = 300 (R/R_c)^{-3/4} \text{ eV}$ .

## Cygnus X-1, RXTE, October 23, 1996

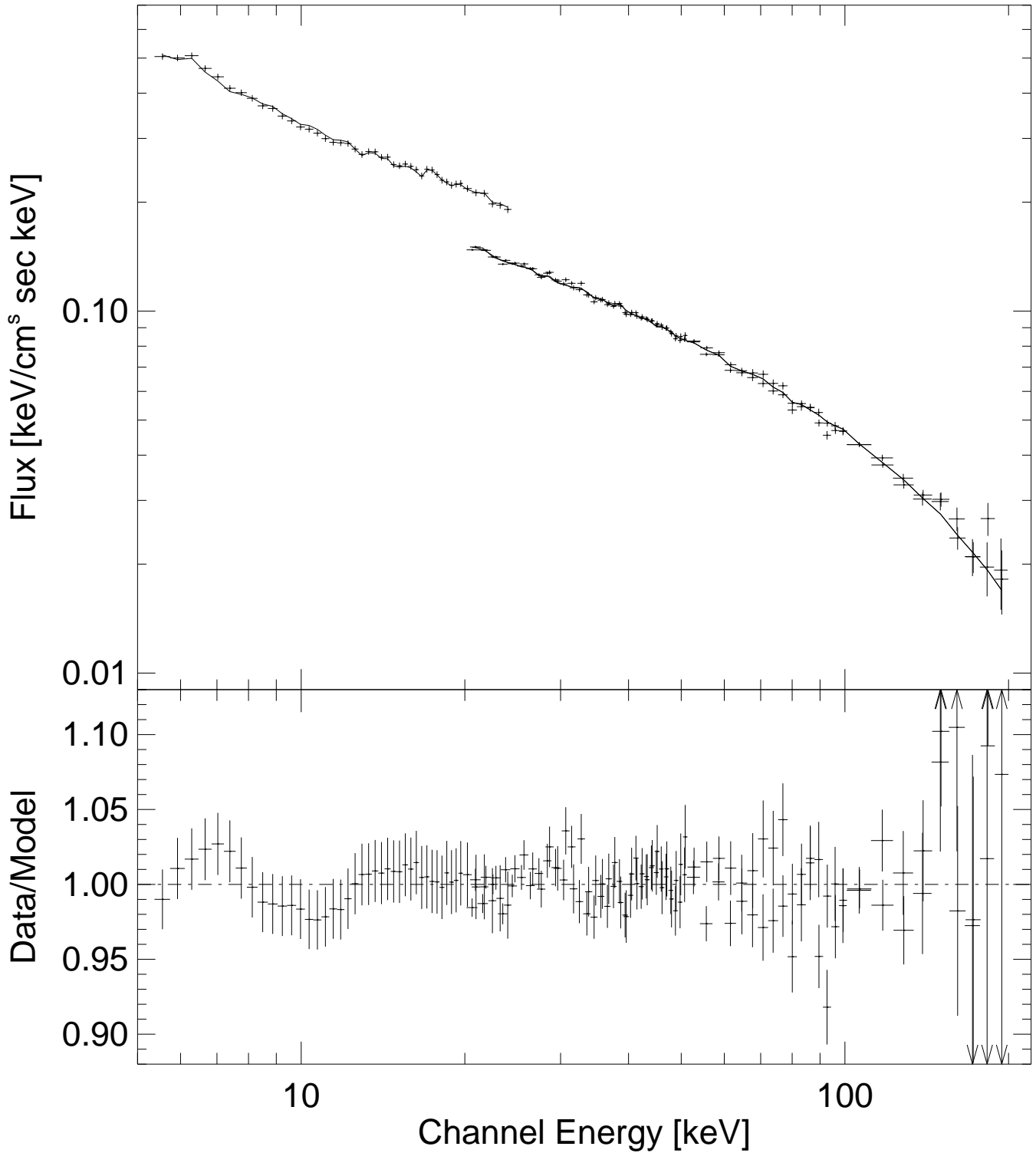


FIG. 1.— Top: Best-fit sphere+disk fit to the PCA and HEXTE data. The jump between PCA and HEXTE is due to the uncertainty in the effective areas of the instruments (see text). Bottom: Ratio between data and model for the best-fit sphere+disk model. Deviations less than 2% are within the range of uncertainty of the PCA response matrix.